JOURNAL OF BACTERIOLOGY, July 2005, p. 4689–4697 Vol. 187, No. 14
0021-9193/05/$08.00+0 doi:10.1128/JB.187.14.4689–4697.2005

Escherichia coli HypA Is a Zinc Metalloprotein with a Weak Affinity for Nickel

Anelia Atanassova and Deborah B. Zamble*

Department of Chemistry, University of Toronto, Lash Miller Chemical Laboratories, 80 St. George St., Toronto, Ontario M5S 3H6, Canada

Received 17 February 2005/Accepted 5 April 2005

The *hyp* operon encodes accessory proteins that are required for the maturation of the [NiFe] hydrogenase enzymes and, in some organisms, for the production of urease enzymes as well. HypA or a homologous protein is required for nickel insertion into the hydrogenase precursor proteins. In this study, recombinant HypA from *Escherichia coli* was purified and characterized in vitro. Metal analysis was used to demonstrate that HypA simultaneously binds stoichiometric Zn^{2+} and stoichiometric Ni^{2+}. Competition experiments with a metallochromic indicator reveal that HypA binds zinc with nanomolar affinity. Spectroscopic analysis of cobalt-containing HypA provides evidence for a tetrathiolate coordination sphere, suggesting that the zinc site has a structural role. In addition, HypA can exist as several oligomeric complexes and the zinc content modulates the quaternary structure of the protein. Fluorescence titration experiments demonstrate that HypA binds nickel with micromolar affinity and that the presence of zinc does not dramatically affect the nickel-binding activity. Finally, complex formation between HypA and HypB, another accessory protein required for nickel insertion, was observed. These experiments suggest that HypA is an architectural component of the hydrogenase metallocenter assembly pathway and that it may also have a direct role in the delivery of nickel to the hydrogenase large subunit.

Hydrogen metabolism is important in a variety of organisms that either consume hydrogen gas as an alternative source of energy or produce it in the dispersion of excess reducing equivalents (10, 22, 42, 48). A key enzyme in these pathways is hydrogenase, which catalyzes the reversible formation of H_2 from protons and electrons (15, 42). The mechanisms of action and the structures of hydrogenases have been extensively studied due to their unusual chemistry, as well as the potential for use in biotechnological applications (for examples of recent reviews, see references 10, 15, 22, and 49). The hydrogenases can be divided into three phylogenetically distinct classes on the basis of the active-site composition (48). Members of one of these classes, the [NiFe] hydrogenases, are widely distributed in *Bacteria* and *Archaea* (48) and contain one iron and one nickel in a deeply buried bimetallic active site (49).

Biosynthesis of the [NiFe] hydrogenase molecular structures in vivo requires multiple accessory proteins that sequentially assemble and insert the active-site components (6, 12, 28, 39, 48). These proteins have been assigned the hydrogenase pleiotropy (Hyp) designation in many organisms. Although the details of hydrogenase metallocenter assembly are not yet clear, the sequence of events has been mapped out based on genetic and biochemical studies of several systems, including the biosynthesis of *Escherichia coli* hydrogenase 3. In the first phase, HypCDEF interact with the hydrogenase large subunit to prepare and insert the iron center with its unusual three CO and CN diatomic ligands. HypC then remains associated with the precursor protein to facilitate GTP-dependent nickel insertion by several other accessory factors. The final steps involve nickel-dependent proteolytic processing of a carboxyl-terminal fragment, internalization of the metallocenter, and association with the small subunit to produce active enzyme.

Studies of the [NiFe] hydrogenase maturation pathways in *E. coli* and *Helicobacter pylori* demonstrate that nickel insertion is accomplished by the cooperative efforts of several accessory proteins. HypA and HypB are implicated in this step of the production of hydrogenase 3 from *E. coli* and the *H. pylori* hydrogenase because lesions in either gene result in an enzymatic deficiency that is partially complemented by the addition of excess nickel to the growth medium (24, 26, 31, 34, 41, 52). The maturation of the other *E. coli* isoenzymes, hydrogenases 1 and 2, also requires HypB, but HypA is replaced by the homologous protein HybF (24). Finally, a recent study demonstrated that the peptidyl-prolyl isomerase SlyD interacts with HypB and is required for the optimal production of all three hydrogenases in *E. coli* (54).

It is not clear what roles these accessory proteins play or how they cooperate to insert nickel into the hydrogenase precursor proteins. GTP hydrolysis is catalyzed by HypB (33, 34, 38), but although HypB proteins from *Bradyrhizobium japonicum* and *Rhizobium leguminosarum* are nickel-binding proteins (16, 43), nickel was not detected in HypB from *E. coli* or *H. pylori* (33, 38). SlyD can bind multiple nickel ions (23); however, the Δ*slyD* strain of *E. coli* only has a partially deficient hydrogenase phenotype (54), suggesting that this protein is not the key nickel delivery factor. Instead, it has been proposed that HypA/HybF might serve as a source of nickel in *E. coli* and *H. pylori* at low metal concentrations (7, 38).

In order to understand more about the cellular functions of these proteins, we purified *E. coli* HypA and examined the biochemical properties of this protein. While this work was in

* Corresponding author. Mailing address: Department of Chemistry, University of Toronto, Lash Miller Chemical Laboratories, 80 St. George St., Toronto, Ontario M5S 3H6, Canada. Phone and Fax: (416) 978-3568. E-mail: dzamble@chem.utoronto.ca.

```
HYPA_ECOLI      MHEITLCQRA LELIEQQAAK HGAKRVTGVW LKIGAFSCVE TSSLAFCFDL VCRGS-VAEG
HYPA_AZOVI      MHEMSIAEGI VQLLEEQAVA QDFTRVRALW LEIGPLAAIE VESLRFCFEA VTRGS-LAEG
HYPA_BRAJA      MHEMALCEGI IGIVEEEARK RAFAKVNVVC LEIGALSHVA PEALQFCFEA VAART-IAQG
HYPA_HELPY      MHEYSVVSSL IALCEEHAKK NQAHKIERVV VGIGERSAMD KSLFVSAFET FREESLVCKD
HYBF_ECOLI      MHELSLCQSA VEIIQRQAEQ HDVKRVTAVW LEIGALSCVE ESAVRFSFEI VCHGT-VAQG
HYBF_KLEPN      MHELSLCMSA ADIIREQAEQ HGIARVTDVW LEVGALADVE ESALHFCFDI ACRDT-VAQG
                *** ::       : ...*   .   ::  :  : :*  : :   . .  .*:      : :.:.

HYPA_ECOLI      CKLHLEEQEA ECWCETCQQY VTLLTQRVRR CPQCHGDMLQ IVADDGLQIR RIEIDQE
HYPA_AZOVI      ARLEIVELPG RAWCLGCNAS VAI-RRRYDA CPQCGSHRLQ VTQGDELRVK ELEVE--
HYPA_BRAJA      AKLEIVETPG TAWCMACSKS VEI-KQRYEP CPSCGGYQLQ VTGGEEMRVR ELEVD--
HYPA_HELPY      AILDIVDEKV ELECKDCSHV FKPNALDYGV CEKCHSKNVI ITQGNEMRLL SLEMLAE
HYBF_ECOLI      CDLHIVYKPA QAWCWDCSQV VEI-HQHDAQ CPLCHGERLR VDTGDSLIVK SIEVE--
HYBF_KLEPN      CTLHIDVIPA QAWCWDCSRE AEI-MQHAGC CPHCGSERLR ITEGDDLRVK SLEGE--
                . *.:       *  *.              *  * .  :  :  .: : :   :*
```

FIG. 1. Alignment of representative HypA protein sequences from *E. coli* (ECOLI), *Azotobacter vinelandii* (AZOVI; 36% identical and 52% similar), *Bradyrhizobium japonicum* (BRAJA, 35% identical and 57% similar), and *H. pylori* (HELPY; 22% identical and 42% similar). HybF sequences from *E. coli* (48% identical and 70% similar) and *Klebsiella pneumoniae* (KLEPN; 42% identical and 65% similar) are also shown. This figure was generated by using ClustalW, and the homology listed is with the *E. coli* HypA sequence. All of the conserved His and Cys residues are in bold. Experiments with *E. coli* HybF and *H. pylori* HypA revealed that H2 is required for nickel binding (7, 38), and it was proposed that the four conserved cysteines are the zinc ligands in HybF (7). Symbols: *, identity; :, strong similarity; ., weak similarity.

progress, two studies of HypA homologs (Fig. 1) were reported. In vitro analysis of *H. pylori* HypA revealed that it forms a homodimer that cooperatively binds two nickel ions and that the protein can associate with HypB (38). A Strep tag fusion of HybF from *E. coli* also binds nickel and/or zinc, but neither dimerization nor association with HypB was detected (7).

The present study of *E. coli* HypA demonstrates clearly that the protein has two distinct metal-binding sites, a high-affinity Zn^{2+} site and a lower-affinity Ni^{2+} site. Examination of these metal-binding sites reveals that the zinc site has the properties of a structural cofactor and that it influences the quaternary structure of the protein. Nickel binding is independent of zinc, suggesting that the two sites have separate functions in the activity of HypA. Furthermore, in vitro cross-linking studies demonstrate the formation of a heterodimer between HypA and HypB that is not modulated by nickel. These studies provide a complete picture of the metal-binding activities of HypA and lead to a discussion of the possible roles of HypA in hydrogenase metallocenter assembly.

MATERIALS AND METHODS

Materials. Competent *E. coli* XL2-blue cells were obtained from Stratagene. Restriction endonucleases were from New England BioLabs. The rapid DNA ligation kit was from MBI Fermentas. HiTrapQ HP 5-ml anion-exchange columns and Superdex 75 gel filtration resin were from Amersham Pharmacia Biotech, the Ni(II)-nitrilotriacetic acid (NTA) agarose resin was purchased from QIAGEN, and Chelex 100 resin was purchased from Bio-Rad. Metal salts were a minimum of 99.9% pure and were purchased from Aldrich. Metal-binding studies were performed with atomic absorption standard solutions from Avery, and these were also used as standards for metal analysis. Other reagents were analytical grade from Sigma. Buffers for all metal assays were treated with Chelex 100 to minimize trace metal contamination. All the samples were prepared with Milli-Q water (18.2 MΩ-cm resistance; Millipore). Anti-HypB polyclonal serum (33) was a generous gift from A. Böck, University of Munich, Munich, Germany.

Cloning, expression, and purification. The *hypA* gene was amplified by PCR from genomic DNA of *E. coli* DH5α by using the primers 5′-GGAGGC**CATATG**CACGAAATAACCCTCTGC and 5′-GTTGTACA**CTCGAG**TCACTCCTGGTCTATTTC (boldface type and underlining indicate restriction sites and the start codon, respectively). The PCR product (351 bp) was digested with NdeI and XhoI, ligated into the pET24b vector (Novagen) cut with the same enzymes, and transformed into DH5α. DNA sequencing (ACGT, Toronto, Ontario, Canada) was used to verify the fidelity of the isolated DNA. The expression vector was then freshly transformed into *E. coli* BL21(DE3). Overnight cultures were used to inoculate LB medium supplemented with 50 μg/ml kanamycin, and the cultures were grown to an optical density at 600 nm of 0.5 at 37°C. The cells were cooled to 15°C and then induced with 0.2 mM isopropyl-β-D-thiogalactopyranoside (IPTG) at an optical density at 600 nm of 0.7 to 0.9. Preliminary experiments demonstrated that the addition of extra Ni^{2+} or Zn^{2+} to the medium led to oligomerization and aggregation of the protein, so they were not added to subsequent preparations. The cells were grown for an additional 20 h at 15°C, harvested, and resuspended in lysis buffer [20 mM Tris (pH 7.5), 100 mM NaCl, 1 mM Tris(2-carboxyethyl)phosphine hydrochloride (TCEP)]. All purification steps were performed on ice or at 4°C. The cells were sonicated and centrifuged at 17,000 rpm for 45 min, and the supernatant was loaded onto a 5-ml HiTrapQ column preequilibrated with 20 mM Tris (pH 7.5)–100 mM NaCl–1 mM TCEP–10% glycerol. The fractions containing HypA were eluted with a linear NaCl gradient, analyzed by 15% sodium dodecyl sulfate-polyacrylamide gel electrophoresis (SDS-PAGE), and pooled. To facilitate more efficient binding to the Ni(II)-NTA resin, 0.1 M NaH_2PO_4 (SPB) at pH 8.0 and 0.3 M NaCl were added. The semipurified protein extract was gently mixed with Ni(II)-NTA slurry (QIAGEN) for 1 h. Unbound proteins were washed from the resin with 50 mM SPB (pH 8.0)–1 M NaCl–1 mM TCEP–10% glycerol. HypA was eluted with 50 mM SPB (pH 8.0)–50 mM imidazole–100 mM NaCl–1 mM TCEP–10% glycerol. The final step of HypA purification was performed on a Superdex 75 column equilibrated with 20 mM Tris (pH 7.5)–100 mM NaCl–1 mM TCEP–10% glycerol, and the protein that eluted at a volume corresponding to a dimer was collected for further studies (discussed below). The purified protein was dialyzed overnight against 20 mM HEPES (pH 7.5)–100 mM NaCl–1 mM TCEP–10% glycerol and stored at −20°C. The identity of the purified protein was confirmed by electrospray ionization mass spectrometry. The molecular mass of the protein was 13,167.8 ± 0.6, which corresponded to the predicted mass (13,168.1 Da) with the initiation methionine still present. The yield of the pure protein from 1.5 liters of culture was typically less than 1 mg. Severalfold higher yields could be achieved if the lysate was loaded onto the Ni(II)-NTA column before the anion-exchange step, but in this case the protein eluted from the gel filtration column at a volume corresponding to a pentamer and the protein was not fully reduced (data not shown).

DTNB assay. The oxidation state of HypA was determined by adding Ellman's reagent, 5,5′-dithiobis(2-nitrobenzoic acid) (DTNB), and monitoring the formation of 5-thio-2-nitrobenzoic acid at 412 nm. The TCEP was removed from the

protein samples on a G-25 gel filtration column prior to analysis. A fresh solution of DTNB (12.5 mM) was prepared in 0.1 M potassium phosphate buffer, pH 8.0. Thiol reactivity of HypA was measured by the addition of protein solution to a mixture containing 100 μM DTNB, 2 mM EDTA, and 6 M urea. The number of reactive cysteines was calculated from a calibration curve generated by using appropriate concentrations of β-mercaptoethanol. When dithiothreitol (DTT) was used in the purification buffers, the level of Cys-SH reduction was lower for both the dimer and the pentamer (data not shown). Therefore, all steps were performed in the presence of 1 mM TCEP unless otherwise indicated. Typically, the dimer was fully reduced whereas the pentamer was approximately 50% oxidized.

Metal analysis. Metal content was determined by using either inductively coupled plasma-atomic emission spectrometry (ICP-AES) or high-performance liquid chromatography (HPLC) analysis. ICP-AES was performed on a Perkin-Elmer Optima 3000 DV system with a 40-MHz free-running generator with a maximal power of 1,500 W, with a pneumatic nebulizer, and with a segmented-array charge-coupled device detector. The plasma gas flow rate was 15 liters min^{-1}, the auxiliary gas flow rate was 0.5 liter min^{-1}, and the nebulizer gas pressure was 0.8×10^5 Pa. The HPLC method for metal analysis is based on separation of the transition metals on an ion-exchange column, IonPac CS5A (Dionex), and postcolumn coupling with 4-(pyridyl-2-azo)-resorcinol (PAR) for quantitative determination at 500 nm (1). The metals were released from the protein by acid hydrolysis. This method requires 10 to 50 μg protein, and the sensitivity is comparable to ICP-AES.

UV-visible spectroscopy, metal release with PMB, and PAR competition. All electronic absorption spectra were collected on an Agilent 8453 spectrophotometer at room temperature. PAR binds transition metal ions in a 2:1 complex, and the absorption of the PAR-metal complexes at 500 nm can be used for quantitative determination of the metal ions in solution (25). Titration of 10 μM HypA with *p*-mercuribenzoate (PMB) in the presence of 100 μM PAR was performed with or without 6 M guanidine hydrochloride in 20 mM HEPES (pH 7.5)–100 mM NaCl–10% glycerol. The absorbance at 500 nm was recorded 10 min after the addition of each aliquot of PMB. A standard curve was generated with zinc atomic absorption standards under the same conditions. In order to estimate the binding affinity of HypA for zinc, a competition experiment was performed. Apo-HypA was titrated into 100 μM PAR and 5 or 10 μM Zn^{2+} in 20 mM HEPES (pH 7.5)–100 mM NaCl–1 mM DTT–10% glycerol. The samples were equilibrated for 15 min at room temperature, and the absorption was monitored at 500 nm. The affinity constant of HypA was obtained from the equation $K_D = (\text{HypA})(\text{PAR}_2\text{Zn}^{2+})/\beta_{\text{PAR}}(\text{HypA} \cdot \text{Zn}^{2+})(\text{PAR})^2$ (50), and $\beta_{\text{PAR}} = 6.0 \times 10^{12}$ M^{-2} (25, 46).

Oligomeric state of HypA. A Superdex 75 column was used to investigate the oligomerization properties of HypA. A standard curve was generated by using bovine serum albumin, egg albumin, trypsinogen, and lysozyme purchased from Sigma. The separation buffer was 20 mM Tris (pH 7.5)–100 mM NaCl–10% glycerol–1 mM TCEP.

Cobalt substitution of HypA. HypA was expressed from the pET24b vector in minimal medium containing 20 mM Na_2HPO_4; 20 mM KH_2PO_4; 20 mM NH_4Cl; 10 mM NaCl; 1 mM $MgSO_4$; 0.4% (wt/vol) glucose; 10^{-5}% (wt/vol) thiamine; 0.00375 mg/ml Fe_2SO_4; 50 μg/ml kanamycin; 100 mg/liter L-Lys, L-Phe, and L-Thr; and 50 mg/liter L-Ile, L-Leu, L-Val, and L-Met. Co^{2+}, to a final concentration of 10 μM, was added to the medium immediately before induction. Purification was performed as described above.

Nickel loading of HypA. To load HypA with Ni^{2+}, HypA was diluted to 10 μM in 20 mM HEPES (pH 7.5)–0.1 NaCl–10% glycerol–1 mM TCEP, and aliquots of 10 mM $NiSO_4$ were added every 5 min at room temperature with gentle shaking, up to about 40 equivalents. The mixture was then diluted 2.5 times with 20 mM HEPES (pH 7.5)–0.1 NaCl–10% glycerol and concentrated to the initial volume by using Millipore MWCO 5,000 Da ultracentrifugal filter devices. Dilution-concentration was repeated several times to remove all the unbound metal from the protein until the eluate had levels of metal that were lower than the detection limit with PAR.

Preparation of apo-HypA. The purified protein was incubated with 10 molar equivalents of PMB for 15 min on ice. An additional 10 equivalents of PMB was added along with 2 mM EDTA, and the reaction mixture was incubated for 15 min at room temperature. The protein was then incubated with 1 mM DTT for 10 min to reverse the mercury-thiolate bond. The protein was dialyzed at 4°C for 2 days against several changes of 20 mM HEPES (pH 7.5)–0.1 M NaCl–10% glycerol–1 mM TCEP.

Cross-linking and Western analysis with HypB. The HypB purification protocol will be described elsewhere. To investigate the HypA and HypB interaction, cross-linking studies were performed with 1-ethyl-3-(3-dimethylaminopropyl)carbodiimide hydrochloride (EDC) (11, 19), a "zero-length" cross-linker that condenses carboxyl groups and primary amines to produce amide bonds. HypA and HypB were mixed in 50 μl of 0.1 M potassium phosphate buffer, pH 6.5, and incubated overnight at 4°C. EDC was added to a final concentration of 5 mM, and the reaction mixture was incubated for 1 h at room temperature. The samples were dried, mixed with SDS-PAGE sample buffer, separated by 15% SDS-PAGE, and stained with Coomassie dye. For Western analysis, the proteins were transferred onto nitrocellulose and probed with the anti-HypB antibody at a 1:1,000 dilution. The secondary antibody, diluted 1:30,000, was a goat anti-rabbit–horseradish peroxidase conjugate (Bio-Rad). The enhanced-chemiluminescence technique (Pierce Biotech, Rockford, IL) was used for detection.

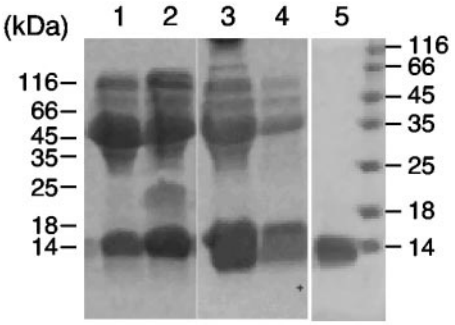

FIG. 2. Purification of HypA induced from a pET expression vector. Fractions collected from sequential HiTrapQ (lanes 1 and 2), Ni(II)-NTA (lanes 3 and 4), and Superdex 75 (lane 5) columns were analyzed by 15% SDS-PAGE. This figure is a composite of several gels.

Circular dichroism (CD) of HypA. CD spectra were monitored on a Jasco J-710 spectropolarimeter by using a cylindrical cell with a 0.1-cm optical path length over a wavelength range of 260 to 205 nm at room temperature. Each CD spectrum was the average of five accumulations at a scanning speed of 50 nm/min, a 1.0-nm spectral bandwidth, a data pitch of 0.1 nm, and a 4-s response time. Apo-HypA (20 μM) in 20 mM HEPES (pH 7.5)–100 mM NaCl–1 mM TCEP–10% glycerol was compared to the same sample incubated with 2 equivalents of Zn^{2+}. The secondary structure was predicted from the primary sequence by using several computer programs available on the ExPASy website (17) including HNN and Jpred (13, 21). Analysis of the experimental data was performed by using the software CDPro (45).

Fluorescence analysis of HypA. Fluorescence measurements were performed on a Perkin-Elmer LS50B luminescence spectrophotometer with FL Win Lab software at 345 nm (excitation, 295 nm), 5-nm slits, and a 0.5-s response time. Apo-HypA (10 μM) was prepared in 20 mM HEPES (pH 7.5)–100 mM NaCl–1 mM TCEP–10% glycerol. For the nickel titrations, the fractional saturation *r* was calculated by using the equation $r = (F_{\text{obs}} - F_{\text{max}})/(F_{\text{min}} - F_{\text{max}})$, the free-nickel concentration was calculated by subtracting the concentration of Ni(II)-HypA from the total nickel concentration, and the data were fitted to the Langmuir equation with a variable Hill coefficient *n*: $r = [\text{Ni(II)}]^n/\{[K_{d(\text{app})}]^n + [\text{Ni(II)}]^n\}$, where $K_{d(\text{app})}$ represents the free-metal concentration required for 50% saturation.

RESULTS

HypA expression and purification. Previous attempts to purify HypA were precluded by the insolubility of the expressed protein (7). Indeed, in the present study induction of *E. coli* HypA expression at 37°C resulted in a strong band on an SDS-PAGE gel that migrated just below the 14-kDa molecular weight marker (HypA has an expected mass of 13,168 Da), but upon cell lysis the protein was only observed in the insoluble fraction (data not shown). Expression of soluble HypA was achieved only when slow protein production was induced at 15°C. The protein could be purified by a sequence of anion-exchange, Ni(II)-NTA, and gel filtration chromatographic steps (Fig. 2). Although binding to the Ni(II)-NTA resin was the first indication that *E. coli* HypA is a weak nickel-binding protein, a high degree of purification was not achieved from

TABLE 1. Metal analysis of HypA

Protein sample[a]	Equivalents of metal/subunit of HypA		
	Nickel	Zinc	Cobalt
Dimer	0.14 ± 0.06	0.7 ± 0.1	ND
Pentamer	ND[b]	0.32 ± 0.07	ND
Apo-HypA + Zn(II)	ND	1.1	ND
Apo-HypA + Ni(II), Zn(II)[c]	1.1 ± 0.2	1.1 ± 0.1	ND
Co(II)-HypA	ND	ND	0.51 ± 0.09

[a] All proteins were expressed in LB without added metal, except for the Co(II) HypA, which was induced in minimal medium containing $CoSO_4$. The results are the averages and standard deviations from at least three trials, except for the addition of only zinc to apo-HypA, which was performed once.
[b] ND, not detected.
[c] Purified HypA dimer was incubated with several equivalents of zinc and a large excess of nickel before washing as described in Materials and Methods.

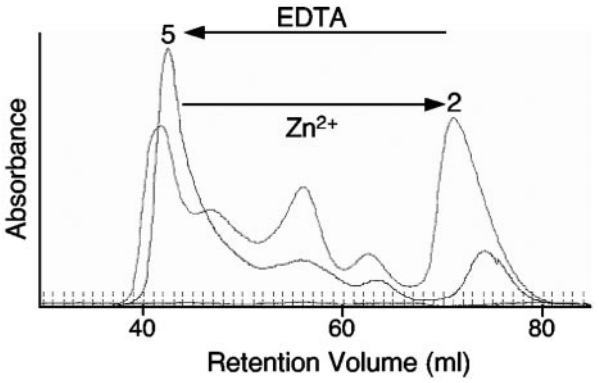

FIG. 3. Gel filtration chromatography of HypA. HypA was treated either with EDTA or Zn(II) prior to loading on the gel filtration column. The numbers indicate pentamer and dimer. The peak eluting following the pentamer is an impurity.

this step because the protein eluted at the low concentration of 50 mM imidazole. However, if the Ni(II)-NTA resin was omitted, then purification was not possible even with additional ion-exchange columns. The elution volume of the purest fractions of HypA from the gel filtration column corresponded to a molecular mass of 26 to 27 kDa, suggesting that HypA is a dimer (data not shown). HypA also eluted at volumes corresponding to other quaternary states, predominantly pentamer (discussed below). The experiments described in this report were performed with the purified dimer unless otherwise noted, and all concentrations listed refer to the concentration of HypA subunits.

HypA characterization. One possible role for HypA in hydrogenase biosynthesis is as a nickel metallochaperone that transfers nickel into the precursor protein. Furthermore, HypA has two pairs of conserved CxxC motifs (Fig. 1), a sequence that is commonly found in zinc metalloproteins (4, 47). To investigate the metal content of HypA, metal analysis was performed by using either ICP-AES or an HPLC assay (1). Analysis of freshly purified protein revealed that the dimer contained approximately 0.7 equivalent of zinc per subunit and 0.1 equivalent of nickel (Table 1), whereas the pentamer contained about 0.3 equivalent of zinc and nickel was not detected. Attempts to prepare protein containing only nickel by expression in minimal medium supplemented with 10 μM $NiSO_4$ resulted in apo-HypA that could not be loaded with zinc and precipitated when incubated with nickel (data not shown). The amount of zinc detected in HypA suggests that there are two zinc ions bound per dimer, but 2 full equivalents were not detected immediately following purification. To rule out a stoichiometry of one zinc ion per dimer, the protein was incubated with several equivalents of zinc, either in the absence or in the presence of excess nickel, followed by washing and metal analysis to reveal approximately one zinc ion per protein monomer (Table 1).

During optimization of the purification procedures, it became apparent that HypA eluted from the gel filtration column in a range of quaternary states and that the oligomerization of HypA was affected by the presence of Zn^{2+} or EDTA in the buffer (Fig. 3), although only monomer was detected by SDS-PAGE (Fig. 2). When the HypA dimer was treated with EDTA, most of the protein eluted at a volume corresponding to a pentamer, whereas if the pentamer was treated with Zn^{2+}, a decrease in the quaternary structure was observed.

Theoretical predictions (13, 21) based on the amino acid sequence of HypA suggest that the protein contains proportional amounts of alpha helices and beta strands. The CD profile of the HypA dimer has a broad absorption that corresponds to a mixture of secondary structures (data not shown) (20), although fitting of the CD data suggests that there is significantly more beta sheet than helices (45). The spectrum of the apoprotein was similar except for a decrease in ellipticity at the shorter wavelength, indicating a less organized structure (data not shown), and no significant change in the secondary structure was observed upon addition of nickel.

Zinc binding to HypA. A recent study of *E. coli* HybF, a HypA homolog, revealed that this protein also binds stoichiometric zinc (7). It was suggested that the conserved CxxC sequences were involved in zinc binding, but the zinc site was not characterized. To determine if the zinc coordination sphere of HypA contains cysteine thiolates as predicted, the HypA dimer was titrated with the organomercurial compound PMB to trap the cysteine thiols by mercuration. The displaced zinc was detected with the metallochromic indicator PAR, which binds Zn^{2+} in a 2:1 complex with strong absorbance at 500 nm (25), and the amount of metal released was estimated by comparison with a Zn(II) standard curve. Partial zinc release was observed if HypA was incubated with PAR alone, indicating that under these conditions HypA had a similar affinity for zinc as PAR (Fig. 4 and discussed below). Upon titration of HypA with PMB, the absorbance at 500 nm increased monotonically until 10 molar equivalents had been added (Fig. 4). The amount of PMB-released metal was equivalent to the total amount determined by ICP and HPLC metal analyses, 0.6 to 0.7 equivalent of zinc and only trace amounts of nickel. This experiment indicates that all 10 cysteines of HypA are available to form a PMB-mercaptide bond and that at least 1 of the cysteines is a zinc ligand. A similar titration curve was obtained in the presence of 6 M guanidine hydrochloride (data not shown), indicating that the denaturant did not disrupt zinc binding to HypA.

A common method for examining the nature of zinc-binding sites is to replace the spectroscopically silent Zn(II) ion with cobalt because the electronic absorption spectra of cobalt-substituted proteins are indicative of the geometry and type of

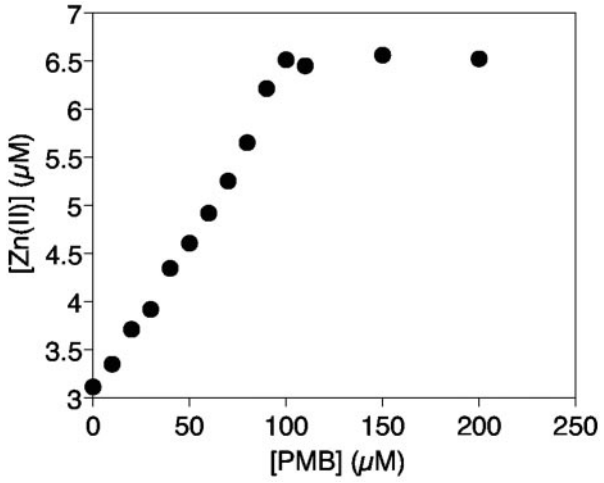

FIG. 4. PMB titration of HypA. HypA (10 μM) in 20 mM HEPES (pH 7.5)–100 mM NaCl–10% glycerol–0.1 mM PAR was titrated with PMB at room temperature. The absorbance was measured 10 min after the addition of each equivalent of PMB. The concentration of metal released was determined by comparing the absorbance at 500 nm to a Zn(II) standard curve.

metal ligands (5, 35). Cobalt-containing HypA was prepared by expressing the protein in minimal medium containing 10 μM $CoSO_4$. Metal analysis of cobalt-substituted HypA revealed, on average, approximately 0.5 equivalent of cobalt per subunit (Table 1), an amount of metal comparable to that observed in the zinc-substituted protein expressed in LB medium. The difference spectrum of cobalt-substituted HypA was generated by subtracting the spectrum of the zinc-containing HypA from the cobalt-loaded protein, revealing absorption bands with energies and intensities that are indicative of a tetrathiolate coordination sphere (Fig. 5) (5). The band at 325 nm is characteristic of $S^- \rightarrow Co(II)$ ligand-to-metal charge transfer, and the extinction coefficient of ~4,600 M^{-1} cm^{-1} indicates that there are probably four thiolate ligands, based on an estimate of 900

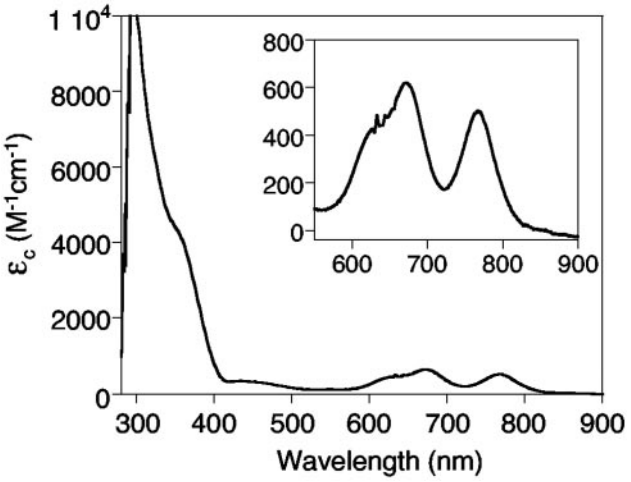

FIG. 5. Electronic absorption spectrum of Co^{2+}-substituted HypA. The spectrum was generated by subtracting the spectrum of zinc-containing HypA and corrected for the Co^{2+} content of this sample as determined by metal analysis (0.6 equivalent).

to 1,300 M^{-1} cm^{-1} per Co-S bond (30, 37). The absorption bands from 500 to 800 nm are due to the d-d electronic transitions (5), and the three peaks with maxima at 634 nm, 672 nm, and 771 nm, with extinction coefficients of >300 M^{-1} cm^{-1}, are similar to those observed in other proteins containing a CoS_4 tetrahedral or distorted tetrahedral coordination environment (18, 27, 29, 44, 53).

To measure the affinity of HypA for zinc, zinc binding was monitored by changes in intrinsic tryptophan fluorescence. *E. coli* HypA contains two tryptophans, one of which, W72, is beside C73 of the first CXXC motifs (Fig. 1). Excitation of apo-HypA at 295 nm yielded a maximum fluorescence at 345 nm that increased upon addition of Zn^{2+}, indicating a zinc-induced change in the tryptophan environment (Fig. 6A and B). The saturation of the fluorescence upon addition of 1 equivalent of metal indicated that the affinity of HypA for zinc is too strong to measure by direct titration, so a competition assay was performed with PAR (Fig. 6C). At pH 7.5, PAR forms 1:1 and 2:1 complexes with Zn^{2+} with affinity constants of 9.7×10^6 and 6.1×10^5 M^{-1}, respectively (25, 46), corresponding to a β_{PAR} of 6.0×10^{12} M^{-2}. Titration of apo-HypA into a solution of zinc and an excess of PAR revealed that HypA can compete with PAR and binds stoichiometric zinc with a K_D of 0.9 ± 0.7 nM.

Nickel binding to HypA. As mentioned above, in addition to zinc we routinely detected substoichiometric amounts of nickel after purification of the HypA dimer (Table 1). Traces of nickel could be due to adventitious nickel contamination from the Ni(II)-NTA column. However, another possibility is that there is a weak nickel-binding site on HypA, in analogy with *E. coli* HybF and *H. pylori* HypA, both of which bind nickel with micromolar affinity (7, 38). To test whether *E. coli* HypA also binds stoichiometric nickel, up to 40 equivalents of nickel were slowly titrated into HypA, followed by multiple ultrafiltration washes until no metal was detected in the flowthrough. Metal analysis revealed stoichiometric nickel, while the amount of zinc detected (60%) was not affected (data not shown). If the protein was incubated with several equivalents of zinc before the addition of excess nickel, then 1 equivalent of each metal was detected bound to HypA (Table 1). The fact that stoichiometric zinc could be detected in the same protein sample as nickel demonstrates that there are two metal-binding sites on HypA and that the large excess of nickel cannot displace the tightly bound zinc.

The affinity of this nickel ion for the HypA dimer was measured by using tryptophan fluorescence. In these experiments, the fluorescence intensity decreased as nickel was titrated into apo-HypA, and saturation was observed only after the addition of about 35 equivalents of nickel (Fig. 7). Half-maximal saturation was observed at 6×10^{-5} M nickel either in the presence or in the absence of 1 equivalent of zinc, demonstrating that filling the zinc site on HypA does not affect nickel binding. The data were best fitted with a small Hill coefficient of 1.2 to 1.3, indicating much less cooperativity than previously observed for the HypA dimer from *H. pylori* (38).

Heterodimer formation. Previous genetic studies demonstrated that HypB and either HypA or HybF are required to produce active hydrogenase in the absence of added nickel (24, 26, 31, 41), suggesting that these proteins cooperate to facilitate the nickel insertion step of hydrogenase metallo-

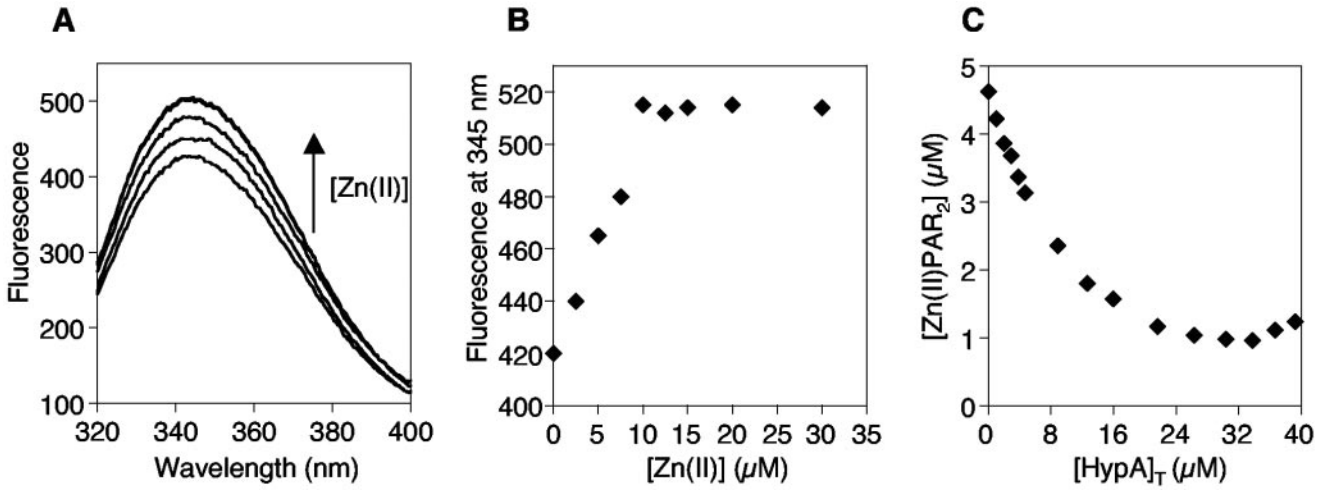

FIG. 6. Apo-HypA titration with Zn(II). (A) Selected fluorescence spectra of 10 μM apo-HypA in 20 mM HEPES (pH 7.5)–100 mM NaCl–1 mM TCEP–10% glycerol titrated with 0 to 20 μM Zn(II). (B) Fluorescence at 345 nm from zinc titration data such as that shown in panel A. (C) Apo-HypA was titrated into a solution of 100 μM PAR–4.6 μM Zn(II). The concentration of $Zn(II)PAR_2$ was determined by comparing the absorbance at 500 nm to a standard curve. A K_D of 0.9 ± 0.7 nM was estimated as described in Materials and Methods from several experiments such as that shown.

center assembly. This hypothesis was supported by in vitro experiments with *H. pylori* proteins demonstrating that HypA forms a heterodimer with HypB (38). However, complex formation between the *E. coli* HybF and HypB proteins was not observed (7). To test if *E. coli* HypA interacts directly with HypB, in vitro cross-linking experiments were performed. Cross-linking of HypB alone produces a higher-molecular-weight band that corresponds to a homodimer (33, 54). Upon incubation of HypA and HypB with EDC, a band corresponding to the molecular weight of the heterodimer was observed (Fig. 8A). The presence of HypB in this complex was confirmed by Western analysis (Fig. 8B). The addition of excess nickel did not affect the formation of this complex (Fig. 8). The HypA-HypB heterodimer was also observed by gel filtration chromatography. Injection of purified HypA and HypB together resulted in a new peak that eluted before either of the isolated proteins, and analysis of this peak by SDS-PAGE revealed the presence of both HypA and HypB (data not shown). Finally, no complex was detected in cross-linking experiments between HypA and SlyD, the other protein implicated in the nickel insertion step of hydrogenase metallocenter assembly (54) (data not shown).

DISCUSSION

HypA is an essential factor for the biosynthesis of hydrogenase 3 in *E. coli* grown under standard anaerobic conditions (26, 31). That the enzyme deficiency of the *hypA* mutant could be partially restored by growing the bacteria in the presence of high concentrations of nickel indicated that HypA was one of the components of the nickel insertion complex (24). In an effort to understand the function of HypA in this complex, we have expressed and purified the protein. The purification of HypA was greatly hindered by poor expression levels, insolubility, and a variable quaternary structure. The predominant oligomers observed on the gel filtration column corresponded to dimers and pentamers. Although the native quaternary structure of HypA is not known, the fact that the dimer was fully reduced suggested that it is more relevant than the oxidized pentamer, so our experiments were performed with the purified dimer.

Metal analysis and competition experiments reveal that *E. coli* HypA has a tightly bound zinc ion. In addition, spectroscopic analysis of the cobalt-containing protein indicates that the metal has four cysteine ligands arranged in a tetrahedral coordination sphere. This result is not surprising given the two highly conserved CxxC motifs present in HypA and its homologues (Fig. 1), because this is a common sequence of tetrathiolate zinc sites (4, 47). Furthermore, the extensive literature on zinc-containing proteins has established that the coordination sphere around the metal ion corresponds to the function of the zinc as a structural, catalytic, or regulatory cofactor (2). A tetrathiolate zinc is usually a structural prosthetic group and is found in several enzymes, as well as many zinc-stabilized structural domains such as zinc finger, RING, LIM, and GATA (4, 47). In a recent study of HybF, in vivo analysis of individual mutations of the CxxC cysteines resulted in poor expression levels and little reduction of the activities of hydrogenases 1 and 2 (7). These observations, in combination with our in vitro studies, support a structural role for the zinc metal cofactor in HypA and HybF.

In proteins with a structural zinc cofactor, the metal ion controls the local conformation and produces a defined structure that modulates interactions with other biomolecules, and many mediate the protein-protein interactions required for the formation of multiprotein complexes (8, 14, 32, 36). In analogy, the zinc-binding domain of HypA could serve as a scaffold for the nickel insertion complex during hydrogenase metallocenter assembly. One explanation for the simultaneous expression of both HypA and HybF in *E. coli*, as previously suggested (7), is

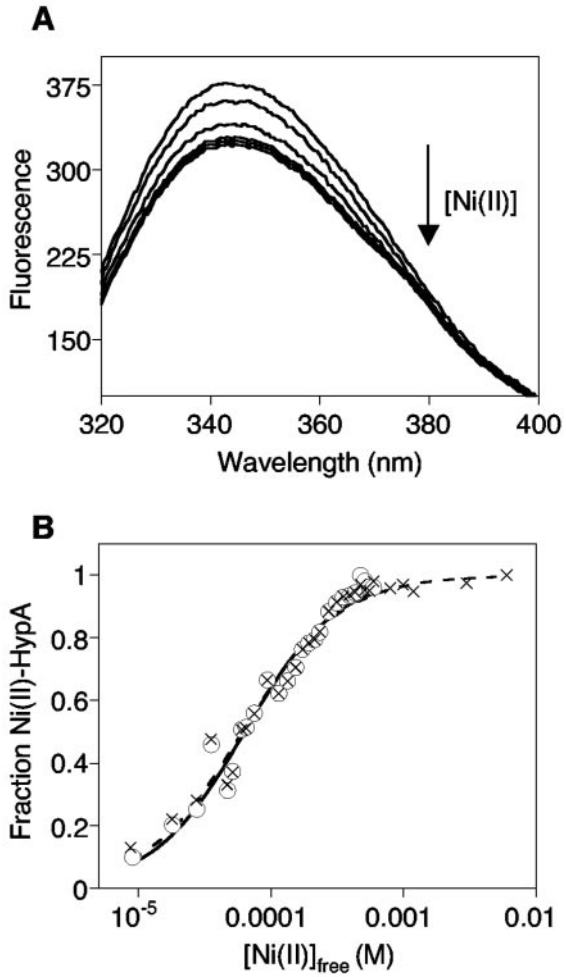

FIG. 7. Fluorescence analysis of HypA titrated with Ni^{2+}. (A) Selected fluorescence spectra of 10 μM HypA in 20 mM HEPES (pH 7.5)–100 mM NaCl–1 mM TCEP–10% glycerol titrated with 0 to 400 μM Ni(II). (B) The fluorescence signals at 345 nm from nickel titrations such as that shown in panel A were fitted to the Hill equation as described in Materials and Methods. Titration of apo-HypA (open circles, solid line) generated an apparent K_D of $6.3 \pm 0.3 \times 10^{-5}$ M and a Hill coefficient of 1.3, and the titration in the presence of 1 equivalent of zinc (crosses, dashed line) resulted in an apparent K_D of $6.1 \pm 0.3 \times 10^{-5}$ M and a Hill coefficient of 1.2.

that two distinct proteins are required to guide the nickel insertion complex to the individual hydrogenase precursor proteins. It is feasible that recognition of hydrogenase 3 would require a separate protein because it has a very different sequence from that of the other two hydrogenase isoenzymes expressed in *E. coli* (48). Further experiments will determine if there is a direct interaction between HypA or HybF and the respective hydrogenase large subunits.

In addition to a high-affinity site for zinc, HypA also separately binds nickel. The two metal-binding sites are at least weakly selective for the appropriate metal because preincubation with multiple equivalents of both nickel and zinc resulted in a single equivalent of each metal bound. Furthermore, the affinity for nickel measured in fluorescence titration experiments was the same for apo-HypA or zinc-containing HypA, indicating that nickel binding is not substantially influenced by the presence of zinc. These experiments suggest that the metal-binding sites of HypA are distinct and may have separate functional roles to play in the activity of HypA. The nickel ligands have not been identified; however, it is likely that H2 participates in nickel binding given that this conserved residue is critical for nickel binding in HybF and *H. pylori* HypA (7, 38). The nickel-binding activity is strong enough to permit partial purification on a Ni(II)-IMAC column, and a nickel affinity of 60 μM was estimated from the fluorescence titration experiments. Micromolar binding of stoichiometric nickel was detected in *E. coli* HybF and *H. pylori* HypA (7, 38), as well as other proteins involved in the biosynthesis of nickel enzymes including the urease accessory protein UreE (3, 9), the carbon monoxide dehydrogenase accessory protein CooJ (51), and HypB homologs from species other than *E. coli* (16, 40, 43). It is not yet clear if micromolar nickel binding is an indication of the concentration of free or kinetically labile nickel in the cell, if tighter binding would be observed in the cellular context of the multiprotein nickel insertion complexes, or if this level of affinity is required for the specific function of these proteins.

The observation that HypA forms a complex with HypB supports the hypothesis that these proteins function together to insert nickel into the hydrogenase 3 precursor protein. Cooperation between HypA and HypB was also proposed for the *H. pylori* hydrogenase maturation pathway (38, 41). It is interesting that, in addition to hydrogenase biosynthesis, *H. pylori* HypA and HypB are required for the production of the other nickel-containing protein of this microorganism, the urease enzyme (41), suggesting that together they serve a more general role in nickel homeostasis. Complex formation between *E. coli* HybF and HypB was not detected (7), but whether this result is because of an ineffective cross-linker, the presence of the affinity tag used to purify the protein, or different properties of HypA and HybF is yet to be determined.

There are thus several possible nonexclusive functions of a HypA-HypB complex during hydrogenase biosynthesis. The first is that HypA directs the nickel insertion complex to the hydrogenase large subunit through protein-protein interactions and that HypB donates the nickel. This model is supported by the nickel-binding activity of HypB homologs and, as mentioned above, by the fact that HypA and HybF are required for the biosynthesis of separate hydrogenase isoenzymes in *E. coli*. However, the observation that both HypA and HybF bind nickel supports a second model, in which it is these proteins that insert the nickel and HypB acts as a regulatory switch at one step, such as release of the hydrogenase precursor protein following nickel insertion. It is also possible that the proteins insert nickel in a more cooperative fashion or that nickel binding by HypA is important for a sensing function that detects the properly inserted metal. Further study is clearly needed to determine the biochemical properties and define the function of each component in the nickel insertion complex. It will also be interesting to determine if the proteins have a conserved function in the many other organisms that express the [NiFe] hydrogenase enzymes.

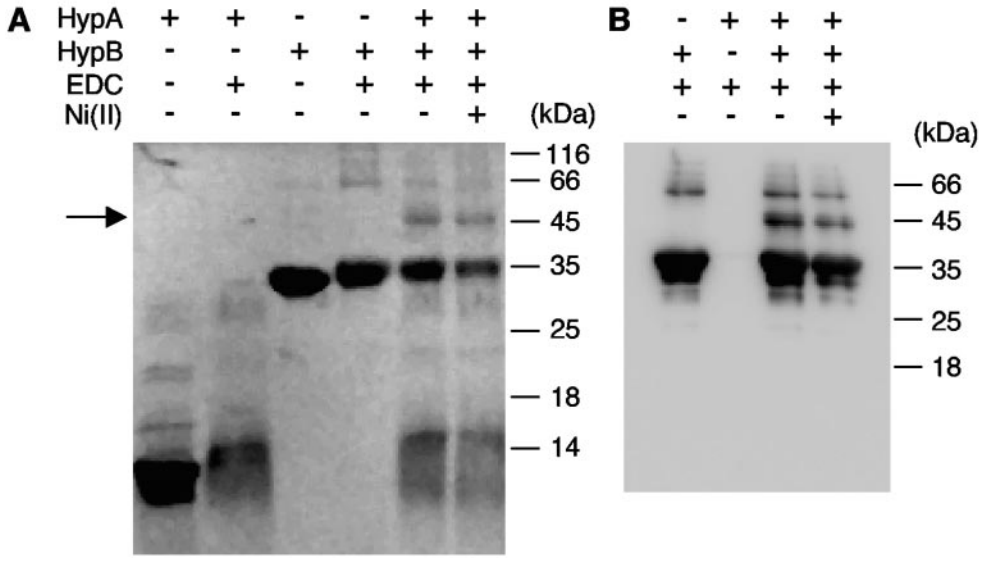

FIG. 8. Formation of the HypA-HypB complex. (A) HypA (10 μM) and/or 5 μM HypB were incubated overnight in 50 μl potassium phosphate buffer, pH 6.5, at 4°C in the presence or absence of 50 μM Ni(II). EDC was added to the indicated samples, followed by an additional 1-h incubation at room temperature. The samples were dried, dissolved in SDS sample buffer, and resolved by 15% SDS-PAGE. (B) An experiment similar to that shown in panel A was used for Western analysis and probed with an anti-HypB antibody.

ACKNOWLEDGMENTS

We thank Michael Leach and Kathleen Zhang for purified HypB and SlyD, Thomas Yoon and Thang Nguyen for technical support, A. Böck for the anti-HypB polyclonal antibody, and M. Nitz for helpful discussions.

This work was supported in part by grants from the Natural Sciences and Engineering Research Council of Canada and the Canada Research Chairs Program.

REFERENCES

1. **Atanassova, A., R. Lam, and D. B. Zamble.** 2004. A high-performance liquid chromatography method for determining transition metal content in proteins. Anal. Biochem. **335:**103–111.
2. **Auld, D. S.** 2001. Zinc coordination sphere in biochemical zinc sites. Biometals **14:**271–313.
3. **Benoit, S., and R. J. Maier.** 2003. Dependence of *Helicobacter pylori* urease activity on the nickel-sequestering ability of the UreE accessory protein. J. Bacteriol. **185:**4787–4795.
4. **Berg, J. M., and Y. Shi.** 1996. The galvanization of biology: a growing appreciation for the roles of zinc. Science **271:**1081–1085.
5. **Bertini, I., and C. Luchinat.** 1984. High spin cobalt(II) as a probe for the investigation of metalloproteins. Adv. Inorg. Biochem. **6:**71–111.
6. **Blokesch, M., A. Paschos, E. Theodoratou, A. Bauer, M. Hube, S. Huth, and A. Böck.** 2002. Metal insertion into NiFe-hydrogenases. Biochem. Soc. Trans. **30:**674–680.
7. **Blokesch, M., M. Rohrmoser, S. Rode, and A. Böck.** 2004. HybF, a zinc-containing protein involved in NiFe hydrogenase maturation. J. Bacteriol. **186:**2603–2611.
8. **Borden, K. L. B.** 2000. RING domains: master builders of molecular scaffolds? J. Mol. Biol. **295:**1103–1112.
9. **Brayman, T. G., and R. P. Hausinger.** 1996. Purification, characterization, and functional analysis of a truncated *Klebsiella aerogenes* UreE urease accessory protein lacking the histidine-rich carboxyl terminus. J. Bacteriol. **178:**5410–5416.
10. **Cammack, R., M. Frey, and R. Robson (ed.).** 2001. Hydrogen as a fuel. Learning from nature. Taylor and Francis, London, England.
11. **Carraway, K. L., and D. E. Koshland.** 1972. Carbodiimide modification of proteins. Methods Enzymol. **25:**616–623.
12. **Casolat, L., and M. Rousset.** 2001. Maturation of the [NiFe] hydrogenases. Trends Microbiol. **9:**228–237.
13. **Cuff, J. A., M. E. Clamp, A. S. Siddiqui, M. Finlay, and G. J. Barton.** 1998. Jpred: a consensus secondary structure prediction server. Bioinformatics **14:**892–893.
14. **Dawid, I. B., J. J. Breen, and R. Toyama.** 1998. LIM domains: multiple roles as adapters and functional modifiers in protein interactions. Trends Genet. **14:**156–162.
15. **Evans, D. J., and C. J. Pickett.** 2003. Chemistry and the hydrogenases. Chem. Soc. Rev. **32:**268–275.
16. **Fu, C., J. W. Olson, and R. J. Maier.** 1995. HypB protein of *Bradyrhizobium japonicum* is a metal-binding GTPase capable of binding 18 divalent nickel ions per dimer. Proc. Natl. Acad. Sci. USA **92:**2333–2337.
17. **Gasteiger, E., A. Gattiker, C. Hoogland, I. Ivanyi, R. D. Appel, and A. Bairoch.** 2003. ExPASy: the proteomics server for in-depth protein knowledge and analysis. Nucleic Acids Res. **31:**3784–3788.
18. **Good, M., and M. Vašák.** 1986. Spectroscopic properties of the Co(II)-substituted α-fragment of rabbit liver metallothionein. Biochemistry **25:**3328–3334.
19. **Grabarek, Z., and J. Gergely.** 1990. Zero-length crosslinking procedure with the use of active esters. Anal. Biochem. **185:**131–135.
20. **Greenfield, N. J.** 1996. Methods to estimate the conformation of proteins and polypeptides from circular dichroism data. Anal. Biochem. **235:**1–10.
21. **Guermeur, Y., C. Geourjon, P. Gallinari, and G. Deléage.** 1999. Improved performance in protein secondary structure prediction by inhomogeneous score combination. Bioinformatics **15:**413–421.
22. **Happe, T., A. Hemschemeier, M. Winkler, and A. Kaminski.** 2002. Hydrogenases in green algae: do they save the algae's life and solve our energy problems? Trends Plant Sci. **7:**246–250.
23. **Hottenrott, S., T. Schumann, A. Plückthun, G. Fischer, and J.-U. Rahfeld.** 1997. *Escherichia coli* SlyD is a metal ion-regulated peptidyl-prolyl *cis*/*trans*-isomerase. J. Biol. Chem. **272:**15697–15701.
24. **Hube, M., M. Blokesch, and A. Böck.** 2002. Network of hydrogenase maturation in *Escherichia coli*: role of accessory proteins HypA and HybF. J. Bacteriol. **184:**3879–3885.
25. **Hunt, J. B., S. H. Neece, and A. Ginsburg.** 1985. The use of 4-(2-pyridylazo)resorcinol in studies of zinc release from *Escherichia coli* aspartate transcarbamoylase. Anal. Biochem. **146:**150–157.
26. **Jacobi, A., R. Rossmann, and A. Böck.** 1992. The *hyp* operon gene products are required for the maturation of catalytically active hydrogenase isoenzymes in *Escherichia coli*. Arch. Microbiol. **158:**444–451.
27. **Johnson, R. S., and H. K. Schachman.** 1983. Communication between catalytic and regulatory subunits in Ni(II) and Co(II)-aspartate transcarbamoylase. J. Biol. Chem. **258:**3528–3538.
28. **Kuchar, J., and R. P. Hausinger.** 2004. Biosynthesis of metal sites. Chem. Rev. **104:**509–526.
29. **Landro, J. A., and P. Schimmel.** 1993. Metal-binding site in a class I tRNA synthetase localized to a cysteine cluster inserted into nucleotide-binding fold. Proc. Natl. Acad. Sci. USA **90:**2261–2265.
30. **Lane, R. W., J. A. Ibers, R. B. Frankel, G. C. Papaefthymiou, and R. H. Holm.** 1977. Synthetic analogues of the active sites of iron-sulfur proteins. 14. Synthesis, properties, and structures of bis(*o*-xylyl-α,α′-dithiolato)ferrate(II, III) anions, analogues of oxidized and reduced rubredoxin sites. J. Am. Chem. Soc. **99:**84–98.
31. **Lutz, S., A. Jacobi, V. Schlensog, R. Böhm, G. Sawers, and A. Böck.** 1991. Molecular characterization of an operon (*hyp*) necessary for the activity of

the three hydrogenase isoenzymes in *Escherichia coli*. Mol. Microbiol. **5:**123–135.
32. **Mackay, J. P., and M. Crossley.** 1998. Zinc fingers are sticking together. Trends Biochem. Sci. **23:**1–4.
33. **Maier, T., A. Jacobi, M. Sauter, and A. Böck.** 1993. The product of the *hypB* gene, which is required for nickel incorporation into hydrogenases, is a novel guanine nucleotide-binding protein. J. Bacteriol. **175:**630–635.
34. **Maier, T., F. Lottspeich, and A. Böck.** 1995. GTP hydrolysis by HypB is essential for nickel insertion into hydrogenases of *Escherichia coli*. Eur. J. Biochem. **230:**133–138.
35. **Maret, W., and B. L. Vallee.** 1993. Cobalt as probe and label of proteins. Methods Enzymol. **226:**52–71.
36. **Matthews, J. M., and M. Sunde.** 2002. Zinc fingers—folds for many occasions. J. Int. Union Biochem. Mol. Biol. **54:**351–355.
37. **May, S. W., and J.-Y. Kuo.** 1978. Preparation and properties of cobalt(II) rubredoxin. Biochemistry **17:**3333–3338.
38. **Mehta, N., J. W. Olson, and R. J. Maier.** 2003. Characterization of *Helicobacter pylori* nickel metabolism accessory proteins needed for maturation of both urease and hydrogenase. J. Bacteriol. **185:**726–734.
39. **Mulrooney, S. B., and R. P. Hausinger.** 2003. Nickel uptake and utilization by microorganisms. FEMS Microbiol. Rev. **27:**239–261.
40. **Olson, J. W., and R. J. Maier.** 2000. Dual roles of *Bradyrhizobium japonicum* nickelin protein in nickel storage and GTP-dependent Ni mobilization. J. Bacteriol. **182:**1702–1705.
41. **Olson, J. W., N. S. Mehta, and R. J. Maier.** 2001. Requirement of nickel metabolism proteins HypA and HypB for full activity of both hydrogenase and urease in *Helicobacter pylori*. Mol. Microbiol. **39:**176–182.
42. **Ragsdale, S. W.** 2000. Nickel containing CO dehydrogenases and hydrogenases, p. 487–518. *In* A. Holzenburg and N. Scrutton (ed.), Enzyme-catalyzed electron and radical transfer, vol. 35. Kluwer Academic/Plenum Publishers, New York, N.Y.
43. **Rey, L., J. Imperial, J.-M. Palacios, and T. Ruiz-Argüeso.** 1994. Purification of *Rhizobium leguminosarum* HypB, a nickel-binding protein required for hydrogenase synthesis. J. Bacteriol. **176:**6066–6073.
44. **Shi, Y., R. D. Beger, and J. M. Berg.** 1993. Metal binding properties of single amino acid deletion mutants of zinc finger peptides: studies using cobalt(II) as a spectroscopic probe. Biophys. J. **64:**749–753.
45. **Sreerama, N., and R. W. Woody.** 2004. Computation and analysis of protein circular dichroism spectra. Methods Enzymol. **383:**318–351.
46. **Tanaka, M., S. Funahashi, and K. Shirai.** 1968. Kinetics of the ligand substitution reaction of the zinc(II)-4-(2-pyridylazo)resorcinol complex with (ethylene glycol)bis(2-aminoethyl ether)-*N*,*N*,*N*′,*N*′-tetraacetic acid. Inorg. Chem. **7:**573–578.
47. **Vallee, B. L., and D. S. Auld.** 1990. Zinc coordination, function, and structure of zinc enzymes and other proteins. Biochemistry **29:**5647–5659.
48. **Vignais, P. M., B. Billoud, and J. Meyer.** 2001. Classification and phylogeny of hydrogenases. FEMS Microbiol. Rev. **25:**455–501.
49. **Volbeda, A., and J. C. Fontecilla-Camps.** 2003. The active site and catalytic mechanisms of NiFe hydrogenases. Dalton Trans., p. 4030–4038.
50. **Walkup, G. K., and B. Imperiali.** 1997. Fluorescent chemosensors for divalent zinc based on zinc finger domains. Enhanced oxidative stability, metal binding affinity, and structural and functional characterization. J. Am. Chem. Soc. **119:**3443–3450.
51. **Watt, R. K., and P. W. Ludden.** 1998. The identification, purification, and characterization of CooJ, a nickel-binding protein that is co-regulated with the Ni-containing CO dehydrogenase from *Rhodospirillum rubrum*. J. Biol. Chem. **273:**10019–10025.
52. **Waugh, R., and D. H. Boxer.** 1986. Pleiotropic hydrogenase mutants of *Escherichia coli* K12: growth in the presence of nickel can restore hydrogenase activity. Biochimie **68:**157–166.
53. **Zamble, D. B., C. P. McClure, J. E. Penner-Hahn, and C. T. Walsh.** 2000. The McbB component of the microcin B17 synthetase is a zinc metalloprotein. Biochemistry **39:**16190–16199.
54. **Zhang, J. W., G. Butland, J. F. Greenblatt, A. Emili, and D. B. Zamble.** 2005. A role for SlyD in the *Escherichia coli* hydrogenase biosynthetic pathway. J. Biol. Chem. **280:**4360–4366.